Measurement of Internal Substrate Binding in Dehaloperoxidase−Hemoglobin by Competition with the Heme−Fluoride Binding Equilibrium

ARTICLE *in* THE JOURNAL OF PHYSICAL CHEMISTRY B · JANUARY 2015

Impact Factor: 3.3 · DOI: 10.1021/jp512996v · Source: PubMed

4 AUTHORS, INCLUDING:

Jing Zhao
North Carolina State University
7 PUBLICATIONS **26** CITATIONS

THE JOURNAL OF PHYSICAL CHEMISTRY B

Article

pubs.acs.org/JPCB

Measurement of Internal Substrate Binding in Dehaloperoxidase−Hemoglobin by Competition with the Heme−Fluoride Binding Equilibrium

Jing Zhao, Justin Moretto, Peter Le, and Stefan Franzen*

Department of Chemistry, North Carolina State University, Raleigh, North Carolina 27695, United States

Supporting Information

ABSTRACT: The application of fluoride anion as a probe for investigating the internal substrate binding has been developed and applied to dehaloperoxidase−hemoglobin (DHP) from *Amphitrite ornata*. By applying the fluoride titration strategy using UV−vis spectroscopy, we have studied series of halogenated phenols, other substituted phenols, halogenated indoles, and several natural amino acids that bind internally (and noncovalently) in the distal binding pocket of the heme. This approach has identified 2,4-dibromophenol (2,4-DBP) as the tightest binding substrate discovered thus far, with approximately 20-fold tighter binding affinity than that of 4-bromophenol (4-BP), a known internally binding inhibitor in DHP. Combined with resonance Raman spectroscopy, we have confirmed that competitive binding equilibria exist between fluoride anion and internally bound molecules. We have further investigated the hydrogen bonding network of the active site of DHP that stabilizes the exogenous fluoride ligand. These measurements demonstrate a general method for determination of differences in substrate binding affinity based on detection of a competitive fluoride binding equilibrium. The significance of the binding that 2,4-dibromophenol binds more tightly than any other substrate is evident when the structural and mechanistic data are taken into consideration.

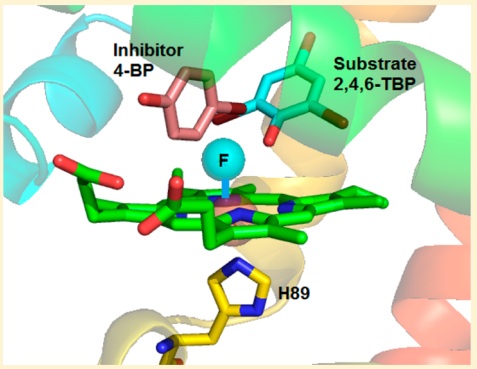

INTRODUCTION

Dehaloperoxidase−hemoglobin (DHP), first isolated from the terebellid polychaete *Amphitrite ornata*, is a multifunctional enzyme that functions as an oxygen transporter,[1] a peroxidase,[2] a peroxygenase,[3] and an oxidase.[3] Oxygen transport is a classical function of hemoglobin that involves reversible dioxygen molecule binding to heme. The binding and release of dioxygen are regulated by the oxygen partial pressure, Bohr effect, and other allosteric effectors in the circulatory system. Although DHP maintains the globin structure, it is of great interest to understand what particular structural determinants lead to its ability to carry out functions other than O_2 transport.[4]

DHP appears to possess a mechanism to incorporate multiple functions into a small protein (15.5 kDa). Although DHP possesses a globin fold and functions as a hemoglobin in *A. ornata*,[1] the peroxidase function[5] was discovered in 1996 and then both peroxygenase and oxidase functions were observed in 2014.[3] To facilitate peroxidase and peroxygenase function in a hemoglobin, much larger molecules than O_2 need to bind to the protein on the surface or in the hydrophobic distal pocket above the heme.[6] Despite the fact that the peroxidase mechanism requires an external binding site, X-ray crystal structures of DHP have shown two distinct internal binding sites for substrate 2,4,6-TXP and inhibitor 4-XP (X = Cl, Br).[7−9] 2,4,6-TBP/2,4,6-TCP binds at α-edge of the heme that deeply buried in the pocket, whereas 4-XP binds right above the heme that right next to the entrance of the distal pocket nearest to the β-edge of the heme. Moreover, with use of protein NMR, the $^1H-^{15}N$ HSQC experiments clearly show that binding of 2,4,6-TCP and 4-BP induces distinct chemical shift patterns and indicates the different binding modes of these two molecules.[10,11] Hydroquinone (H_2Q) was also observed to bind internally in a manner that resembles the inhibitor binding in the distal pocket. H_2Q acts as a peroxidase regulator of DHP by a proton coupled electron transfer (PCET) mechanism.[8] These functions are apparently incompatible with normal globin function, yet DHP does function as a globin as well.[2] To explain this, we propose that there must be a trigger that causes a functional switch in the protein. The simplest model suggests that substrate binding itself is the trigger.[6,12] Thus, experimental measurement of the binding strength and structure of substrates is pivotal for a mechanism that explains the multiple functions.

Aside from the brominated phenols, indole derivatives were recently reported as substrates for the peroxygenase and oxidase functions.[3] Although there are currently no crystal structures of the indole derivatives, it is a reasonable hypothesis that indolic substrates must bind in the distal pocket in proximity to the heme iron to allow the protein carry out either the peroxygenase or oxidase functions.[3] The same site that

Received: October 11, 2014
Revised: January 22, 2015

DOI: 10.1021/jp512996v
J. Phys. Chem. B XXXX, XXX, XXX−XXX

permits peroxygenase function apparently inhibits peroxidase function.[7] This situation has some similarity to indoleamine-2,3-dioxygenase (IDO), which has a large distal pocket and can accommodate substrate in both active and inhibitory conformations.[13] In a multifunctional protein a binding site may serve multiple functions, which is observed in IDO as well.[14] For example, the internal binding site observed for 2,4,6-TCP[9] and 2,4,6-TBP[8] may well be a substrate binding site for the peroxygenase function but an inhibitor site for the peroxidase function. For brevity we will sometimes refer to the internal sites as substrate binding sites, although they may also bind inhibitors. It is important to distinguish the internal mode of binding from the peroxidase substrate binding site, which must be on the surface of DHP, based on the observed radical reactivity of the oxidized substrate under peroxidase conditions.[15,16] Therefore, we call the peroxidase substrate binding site an external site. We can further hypothesize that binding of the various substrates and inhibitors should regulate and possibly permit switching of DHP functions. Thus, it will be extremely useful to find an easy way to quantitatively probe the internal binding of large molecules in DHP. Here we can refer to substrates and inhibitors both as large molecules, which distinguishes them from ligands (such as F^-, CO, O_2, etc.) that are bound to the heme Fe.

Fluoride anion turns out to be an ideal ligand to probe the internal binding of substrates and inhibitors.[17] The advantage of using fluoride anion as a probe the binding affinity of internal binding ligands in DHP is an improvement over H_2O, which naturally binds at the axial position of the ferric heme. The native ferric form of DHP is 60% metaquo (6cHS) and 40% met (5cHS) at pH 6.0. The water binding equilibrium is the reflected by the change of the coordination state of the ferric heme between 6cHS and 5cHS, which can be observed in ν_2 and ν_3 modes in the resonance Raman spectrum.[7,8] These resonance Raman data correlate well with the occupancy of H_2O in the room temperature X-ray crystal structure.[18] This correlation is strengthened by the fact that the distal histidine in the X-ray crystal structure (PDB code 1EW6) has two conformations, one internal that hydrogen-bonds to the H_2O molecule and one external that corresponds to a lack of H_2O and a five-coordinate heme. The 6cHS H_2O is displaced when inhibitors bind in the distal pocket and displace H_2O to form a 5cHS complex, but the signal is small because the H_2O occupancy is only 60%. By replacing H_2O with fluoride anion, one can compare the competitive binding with a ligand that is initially bound to 100% of the heme Fe atoms. The use of fluoride also has the advantage that the assay can be conducted using UV−vis spectroscopy. Fluoride is a weak field ligand, and therefore, there is no change the spin state of the heme iron upon binding. Therefore, the Soret band shows little shift (if any) upon fluoride binding. However, fluoride anion binding can be easily monitored in UV−vis spectra because there is a charge-transfer band CT1 at 605 nm that corresponds to the formation of DHP−F adduct.[19]

In the present study, we have applied the fluoride titration strategy using UV−vis spectroscopy to study the interaction of DHP A with 30 molecules that bind internally (and noncovalently) in the distal binding pocket of the heme. We used resonance Raman spectroscopic methods and density function theory (DFT) calculations to investigate the hydrogen bonding (H-bonding) network of the active site of DHP A as well. By applying the fluoride titration strategy to interrogate the competitive binding interaction between fluoride anion and internally bound molecules, we were able to identify 2,4-DBP as the tightest binding substrate discovered so far. The method also confirmed that the indole derivatives, which were observed to be peroxygenase substrates, bind internally in the distal pocket despite their large size.[3] The trends of the binding affinity of the 5-halogen indole series are consistent with the preliminary mechanistic studies.[20,21] Moreover, the pH-dependent fluoride titration experiment has shown that only the charge neutral form of the substrate bound internally in the distal pocket, as we have surmised previously based on a number of studies.[22−24] The data provide further evidence that DHP is a true multifunctional enzyme.

MATERIAL AND METHODS

Materials. All reagents were purchased from Aldrich and ACROS and used without further purification. All chemicals were each dissolved in 100 mM, pH 7.0, potassium phosphate (KP_i) buffer to prepare the stock solution. 2,4,6-TBP and all halogenated indoles solutions were boiled in the water bath and then cooled to make the supersaturated solutions that meet the concentration requirement. 0.2 and 0.6 M NaF solutions were made in the corresponding KP_i buffer. Spectra were obtained using an Agilent 8453 diode array UV−visible spectrophotometer with a Peltier-cooled sample cell at 25 °C. Wild-type His6X (histidine-tagged) DHP A and H55D mutant were expressed in *E. coli* and purified as previously described.[25,26] The concentration of ferric DHP A was determined by using the molar absorption coefficient, ε = 116 400 M^{-1} cm^{-1}.[27] The Soret band of DHP A H55D mutant is at 398 nm and the corresponding extinction coefficient is 82 500 M^{-1} cm^{-1} determined by the pyridine hemochrome method.[28]

Fluoride Titration Assays. The fluoride titration experiments were conducted using an Agilent 8453 UV−visible spectrophotometer operating in the standard mode. The titrations were carried out in a 0.2 cm path length cuvette obtained from Starna Cells, Inc. The initial ferric DHP A concentration $[E]_0$ in each sample was 50 μM with a total volume of 600 μL. 1 or 5 mM substrates were included for the fluoride competitive binding titration, and the cuvette was allowed to incubate for 3 min in the thermal cell to reach thermal equilibrium before the titration. Then the fluoride stock solution was gradually titrated and the corresponding spectra were recorded. The fluoride titration spectra were eventually normalized according to the protein concentrations in the cuvette. The binding curve was extracted from the spectra region between 300 and 700 nm using SVD (singular value decomposition) and then fitted into the one site reversible binding model to obtain the apparent fluoride binding constant K_d^{app}, which is derived in the following.

Figure 1 shows two noncovalent binding sites called the α- (substrate) and β- (inhibitor) site, as well as the ionic binding site for fluoride with the heme Fe. The X-ray crystal structure data shown in Figure 1 provide one of the motivations for this study. The β-site or inhibitor binding site was observed first in 1999 (PDB code 1EWA)[18] but only defined as an inhibitor site in 2010 (PDB code 3LB2).[7] The name β-site comes from the fact that this binding site is closest to the β-edge of the heme. The α-site was discovered by two research groups using different conditions (PDB code 4HF6 and PDB codes 4KMW and 4KN3)[8,9] and is given its name because the substrate is bound nearest to the α-edge of the heme. On the basis of more recent work, we hypothesize that the α-site is the substrate binding site for the peroxygenase function[3] but is apparently

DOI: 10.1021/jp512996v
J. Phys. Chem. B XXXX, XXX, XXX−XXX

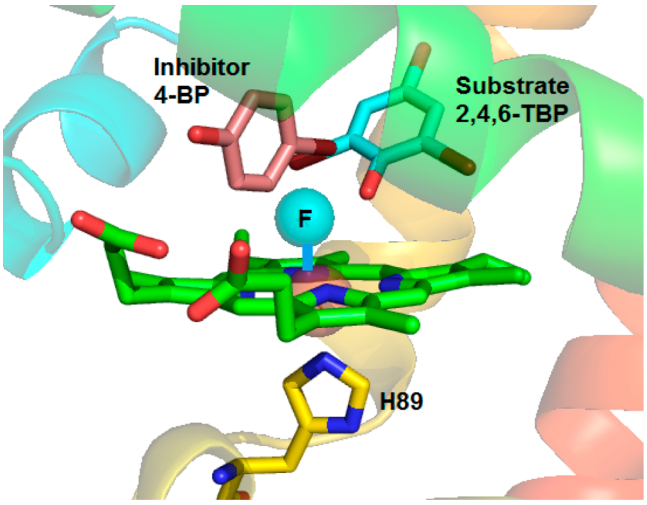

Figure 1. Illustration of two modes of internal binding of substrate 2,4,6-TBP (α-site) and inhibitor 4-BP (β-site) in the distal pocket of DHP A with fluoride coordinated to the heme iron obtained from an overlay of the coordinate files from two X-ray crystal structures of PDB entries 3LB2 and 4HF6, respectively.[7−9]

also a substrate inhibition binding site for the peroxidase function.[8]

Kinetic evidence suggests that DHP binds a number of substrates including halogenated phenols and indoles. Therefore, in order to understand the multiple functions of DHP, it is imperative to characterize the interactions of large molecules in these two binding sites with ligands bound to the heme Fe. There are several possible ligands that could be considered, fluoride, azide, cyanide, etc., for competitive binding studies in ferric DHP. Fluoride was chosen for this study because it has a relatively weak ionic bond that could be relatively easily displaced by noncovalent substrate and inhibitor binding. The competitive binding equilibrium is shown in Scheme 1, in which a square binding equilibrium scheme is used to illustrate the binding interactions between ferric DHP and both fluoride anion and substrates/inhibitors.

According to the square scheme there are four related equilibria. K_L is the dissociation constant for the noncovalent interaction between internal binding molecules (substrates/inhibitors) and ferric DHP. K_d^f denotes the dissociation constant for the ionic bond between fluoride anion and ferric heme in the absence of any internally bound molecule. K_d^b is the dissociation constant between fluoride anion and ferric heme in the presence of an internally bound molecule. We have not included K_d^{app} in the scheme, since it is not a simple equilibrium constant. A detailed derivation of K_d^{app} is given in the Supporting Information, but the following derivation shows the crucial steps needed to obtain the final equation.

Scheme 1. Equilibrium Scheme of Competitive Binding between Fluoride Anion and Internal Binding Substrate or Inhibitor in WT DHP A

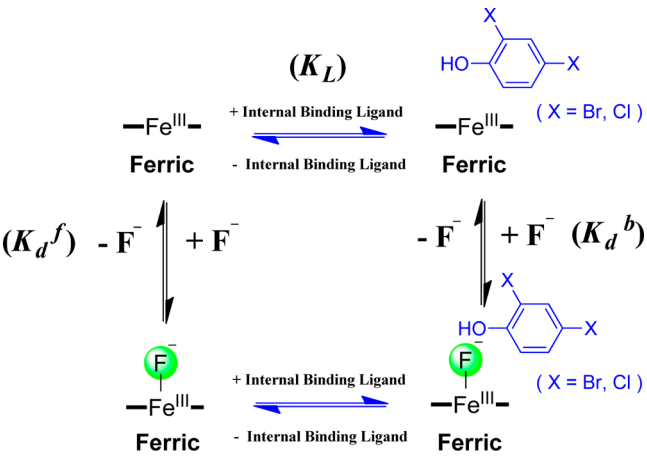

The starting point for the derivation of K_d^{app} is to assume that the enzyme exists in four forms, which are free enzyme, E, substrate-bound enzyme, EL, fluoride bound enzyme, EF, and simultaneous substrate- and fluoride-bound enzyme, EFL (Scheme 1). The mass conservation equation is

$$[E]_0 = [E] + [EL] + [EF] + [EFL] \tag{1}$$

given that $[E]_0$ is the total enzyme concentration. This equation can also be written as

$$[E] = \frac{[E]_0}{1 + \frac{[L]}{K_L} + \frac{[F]}{k_d^f} + \frac{[L][F]}{K_L K_d^b}} \tag{2}$$

Assuming that the fluoride ion concentration is much greater than the enzyme concentration, $[F] \gg [E]_0$, the fluoride binding fraction θ that can be monitored using the UV−vis is

$$\theta = \frac{[EF] + [EFL]}{[E]_0} \tag{3}$$

Substituting in eq 2,

$$\theta = \frac{\frac{[E][F]}{K_d^f} + \frac{[E][L][F]}{K_L K_d^b}}{\left(1 + \frac{[L]}{K_L} + \frac{F}{K_d^f} + \frac{[L][F]}{K_L K_d^b}\right)[E]} \tag{4}$$

A rearrangement of this equation permits it to be written in a standard form for a binding isotherm provided we define an apparent binding constant:

$$\theta = \frac{[F]}{\frac{([L] + K_L)K_d^f K_d^b}{[L]K_d^f + K_L K_d^b} + [F]} = \frac{[F]}{K_d^{app} + [F]} \tag{5}$$

Therefore, we can define the apparent fluoride dissociation constant K_d^{app}:

$$K_d^{app} = \frac{([L] + K_L)K_d^f K_d^b}{[F]K_d^f + K_L K_d^b} \tag{6}$$

As we can see from eq 6, K_d^{app} is dependent on both the concentration of internally bound molecules [L] and the dissociation constant K_L. Because of the presence of competitive binding, K_d^b should be much larger than K_d^f. Therefore, either an increase in the molecular concentration [L] or replacement by a more tight-binding molecule L′ (with smaller dissociation constant $K_{L'}$ value) will drive the fluoride binding equilibrium toward the dissociated form, resulting in an increase in K_d^{app}.

Resonance Raman Spectroscopy. DHP A samples at a final protein concentration of 100 μM were prepared in 100 mM KP_i buffer, pH 7.0. The DHP−F complex was prepared with 0.2 M NaF in the KP_i buffer with corresponding pH (pH 5.0 and pH 7.0). And the DHP−F sample at pD 7.0 was prepared and equilibrated in D_2O. Samples were placed in 5 mm NMR tubes and spun with an air piston spinning sample

DOI: 10.1021/jp512996v
J. Phys. Chem. B XXXX, XXX, XXX−XXX

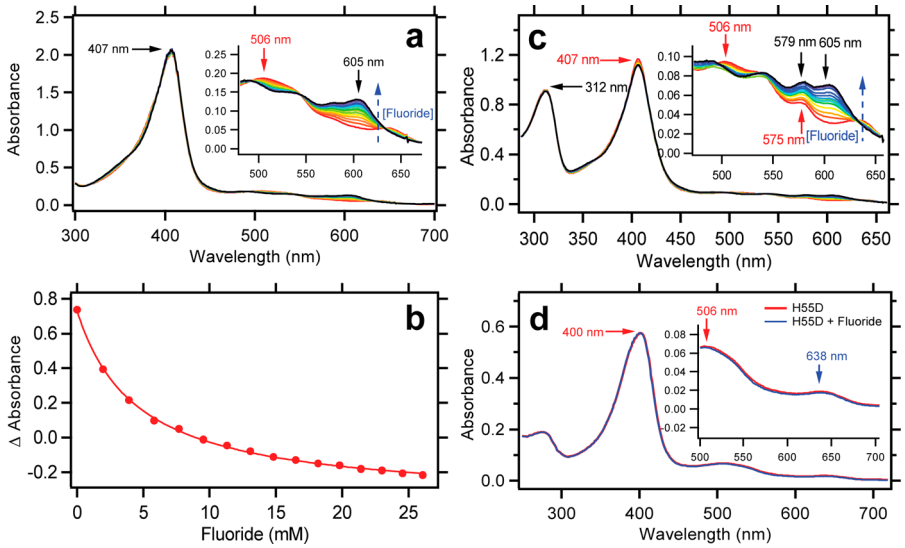

Figure 2. UV−vis spectra of fluoride titration of WT DHP A and DHP A H55D mutant in the absence or in the presence of substrate: (a) fluoride titration of WT DHP A (100 μM) in the 100 mM KP_i buffer, pH 7.0; (b) fluoride binding curve extracted from spectra data of Figure 1a using SVD; (c) fluoride titration of WT DHP A (50 μM) in the presence of 1 mM 2,4,6-TCP in the 100 mM KP_i buffer, pH 7.0; (d) fluoride titration of DHP A H55D mutant (50 μM) in the 100 mM KP_i buffer, pH 7.0; the NaF concentration is up to 0.3 M.

holder (Princeton Photonics, model Raman 101). Resonance Raman spectra were obtained by excitation at the edge of the Soret band at 410 nm. The Coherent Mira 900 tunable titanium sapphire laser generating 700−1000 nm light was pumped by a Coherent Verdi 10 frequency-doubled diode-pumped Nd:vanadate laser generating 10 W of 532 nm light. The near-IR output from the Ti:sapphire laser was sent through a Coherent 5-050 frequency doubler to generate the working range of 400−430 nm light for Soret band excitation. The frequency doubled beam was collimated and cylindrically focused to a vertical line of ~5 mm and typically 90−100 mW at the sample. Raman scattered light was collected by the Spex 1877 Triplemate monochromator (2400 grooves/mm final stage grating) and was detected by a liquid-N_2-cooled CCD camera (ISA Spex, model CCD-3000). Spectra were measured at room temperature for 40 acquisitions with a total exposure time of 1200 s. The spectrograph resolution was determined to be 2.2 cm^{-1} using argon lamp lines. The Raman spectra were first calibrated using standard spectra of toluene, and then baseline subtracted by using a four-point four-polynomial extrapolation and normalized to the intensity of the ν_7 band (see Figure 3).

Density Functional Theory Calculations. Density functional theory (DFT) calculations were conducting using a numerical basis set implemented in the program DMol^3.[29,30] The PBE functional was used.[31] The numerical basis set used is equivalent in quality to a double-ζ basis set with polarization functions on all atoms (DNP). The cutoff used from each atomic center was 20 bohrs. The criterion for convergence was a change less than one part in 10^{-6} for two subsequent iterations of geometry refinement. Fluoride binding energies were carried out using a continuum dielectric for all models. The model chosen is the option COSMO in DMol^3. This model is necessary because of the negative charge on the fluoride and positive charge on all unligated ferric heme models (except those including OH^-).[32] A dielectric constant of 78.4 was used to model room temperature aqueous solvation. Vibrational frequency calculations were carried out by finite difference to construct the force constant matrix. To construct the finite difference forces, each nucleus was shifted six times, along $\pm x$, $\pm y$, and $\pm z$. by 0.1 bohr to obtain an estimate of the second derivative (Hessian), which is also the force constant. The calculations were carried out using the THERMAL option, with the electronic temperature set to 0.005 au (~1500 K).[33] This tool in the DFT method has no physical significance, since a correction to 0 K is implemented when the calculation is completed. However, it helps to ensure convergence in large systems. The systems studied here range from 97 to 109 atoms. The calculations were carried for d^5 ferric Fe in the high spin state so that all of the heme systems are considered to be in the same spin state, consistent with observations by UV−vis spectroscopy.

Using the COSMO dielectric continuum model in the calculation does not describe the solvation of F^- at the molecular level. In order to correct for the specific solvation effect of H_2O on the binding of the F^- ion, the association was carried out using the following equilibrium:

$$\text{heme}^+ + 16H_2O - F^- \rightarrow \text{heme} - F + 16H_2O$$

where heme represents a model that may include proximal histidine and distal amino acid components to represent the hydrogen bonding interactions. The various combinations are given in Tables 4 and 5, and some of these structures are shown in Figure 6. The calculated energy is the energy required to transfer the fluoride ion from the heme Fe atom to solvent, which is modeled using 16 H_2O molecules. The COSMO dielectric continuum was applied to all components of this model.

RESULTS

In this study, we present a competitive binding assay as a general method for determining substrate binding constants needed to understand the nature of internal binding in DHP. Since internal binding corresponds to both substrate and inhibitor binding, these measurements have a direct relationship to the peroxidase, peroxygenase, and oxidase functions of DHP. In previous assays of this type, strong binding ligands, such as CN^-, have been used to displace the substrate (or

DOI: 10.1021/jp512996v
J. Phys. Chem. B XXXX, XXX, XXX−XXX

inhibitor). Instead, the assay used here started with the F^--bound form of the heme, which is then challenged with various concentrations of substrate/inhibitor. There is X-ray crystal structural evidence for both internal inhibitor and substrate binding, and these structures suggest that the large molecules will compete with fluoride binding.[7−9] The competition assay has been developed as a tool to screen for potential new substrates or inhibitors, which may further expand the repertoire of DHP functions.

Fluoride Titration and the Competitive Binding between DHP−F Adduct and the Internal Substrate Binding. The fluoride titration with the WT DHP A and DHP A H55D mutant in the absence or in the presence of substrate was first studied using UV−vis spectroscopy, as shown in Figure 2. The titration of fluoride to WT DHP A does not noticeably change the Soret band, which remains at 407 nm throughout the titration (Figure 2a). In contrast, the Q-band of WT DHP A at 506 nm was gradually diminished and the charge transfer band CT1 at 605 nm increased in intensity, which indicates the formation of the six coordinated high spin (6cHS) fluoride adduct, DHP−F.[34] The fluoride binding curve for the WT DHP A in the absence of substrate is shown in Figure 2b. However, there is an additional band that increases intensity at 579 nm in the presence substrate 2,4,6-TCP (Figure 2c) during the fluoride titration, which may be due to the interaction between internal binding substrate 2,4,6-TCP and the axial fluoride ligand. The H55D mutants showed no binding affinity toward fluoride, since no spectral changes were observed upon adding fluoride to protein solutions (Figure 2d). This result is not a surprise because the distal histidine, H55, is considered to be the crucial H-bond donor that stabilizes the binding of an axial fluoride ligand to the heme Fe atom.[25]

The fluoride anion dissociation constants of both WT DHP A and DHP B have been measured (Table 1). Since these

Table 1. Fluoride Dissociation Constant K_d^f of Several Hemoproteins

hemoprotein	CT1 (nm)	ν_{Fe-F} (cm^{-1})	K_d^f (mM)
WT DHP A	605	461	4.5 ± 0.1
WT DHP B	605	461	4.5 ± 0.4
myoglobin (horse muscle)	607		14.2 ± 0.5
HRP	611	387	61.8 ± 4.9
*Tt*H-NOX[66]	609		1.5 ± 0.2
Tf-trHb[9]	613	381	0.26 ± 0.01
CcP[11]	617		(1.8 ± 0.4) × 10^{-3}

dissociation constants are measured in the absence of aromatic substrates and inhibitors, we denote this dissociation constant as K_d^f. Because of the close similarity of DHP A and DHP B structures and sequences, K_d^f values are nearly identical. In order better understand the distal environment of DHP A and B, we present a comparison of the K_d^f of horse skeletal muscle myoglobin (HSMb) and HRP using the same titration method in this study. HSMb and HRP have ∼3-fold and ∼14-fold weaker binding affinities compared to DHP, while the Tf-trHb and CcP have ∼17-fold and ∼2500-fold stronger binding affinities than DHP, respectively.

The competitive binding between large molecules (L) and fluoride binding to the heme Fe can be quantitatively determined by monitoring the increase of the apparent dissociation constant K_d^{app} given in eq 6 compared to the dissociation constant K_d^f measured in the absence of substrate or inhibitors. Indeed, K_d^{app} did increase in the presence of the substrates and inhibitors (the monohalogenated phenol series) or the classical substrates (the 2,4,6-trihalogenated phenol series) as shown in Table 2. K_d^{app} measured for [L] = 5 mM is

Table 2. Apparent Fluoride Dissociation Constant K_d^{app} of DHP A in the Presence of Internal Binding Molecules

		K_d^{app} (mM)[e]	
internal binding molecule	pK_a(ph-OH)[a]	5 mM	1 mM
4-fluorophenol	9.89[67]	16.2 ± 0.7	7.0 ± 0.3
4-chlorophenol	9.43[67]	22.4 ± 1.1	12.2 ± 0.5
4-bromophenol	9.34[67]	22.9 ± 1.1	12.3 ± 0.8
4-iodophenol	9.20[67]	NA[b]	16.4 ± 0.8
2-bromophenol	8.43[68]	163.4 ± 13.8	25.0 ± 0.6
3-bromophenol	9.03[69]	NA[c]	NA[c]
2,4,6-trifluorophenol	7.20[70]	46.4 ± 4.1	12.7 ± 0.7
2,4,6-trichlorophenol	6.59[71]	NA[b]	14.5 ± 0.8
2,4,6-tribromophenol	6.34[71]	NA[b]	23.8 ± 1.0
2,4-dicholorophenol	8.05[71]	ND	74.1 ± 4.3
2,4-dibromophenol	7.86[71]	ND	172.1 ± 9.0
2,6-dibromophenol	6.89[71]	21.2 ± 1.2	5.7 ± 0.5
phenol	9.97[72]	8.3 ± 0.3	ND
p-cresol	10.15[72]	7.4 ± 0.4	ND
2,3,6-trimethylphenol	10.64[73]	7.7 ± 0.3	ND
p-methoxyphenol	10.20[67]	4.8 ± 0.1	ND
guaiacol	9.93[74]	8.0 ± 0.3	ND
ferulic acid	9.21[75]	8.7 ± 0.3	ND
benzohydroxamic acid	NA	10.7 ± 0.7	ND
L-tryptophan	NA	5.5 ± 0.2	ND
L-phenylalanine	NA	6.6 ± 0.4	ND
L-tyrosine	10.20[76]	NA[d]	10.4 ± 0.6
indole	NA	7.9 ± 0.2	5.0 ± 0.2
5-fluoroindole	NA	NA[d]	5.8 ± 0.7
5-chloroindole	NA	NA[d]	8.6 ± 0.3
5-bromoindole	NA	NA[d]	13.2 ± 0.5
5-iodoindole	NA	NA[d]	16.8 ± 0.4
4-bromoindole	NA	NA[d]	5.2 ± 0.1
6-bromoindole	NA	NA[d]	6.1 ± 0.2
7-bromoindole	NA	NA[d]	6.6 ± 0.2

[a]NA: not available. [b]NA: not available because of protein denaturing. [c]NA: not available because ligand coordinates to the heme. [d]NA: not available because the limit of solubility. [e]ND: not determined.

approximately 2-fold greater than the K_d^{app} measured for [L] = 1 mM. For example, this can be seen for the 4-halogenated phenol series of inhibitors 4-fluoro-, 4-chloro-, or 4-bromophenol. The inhibitor series is the best characterized, which permits us to propose an inverse correlation between the large molecule dissociation constant K_L. K_L follows the trend: 4-IP < 4-BP < 4-CP < 4-FP[7] while K_d^{app} follows the opposite trend (Table 2). The tighter is the binding of the large molecule (i.e., the smaller the K_L), the greater is the corresponding increase in the apparent fluoride dissociation constant (the larger the K_d^{app}). Using this principle, we can estimate the relative K_L by measuring the K_d^{app} using a fluoride titration. The K_d^f of DHP A is 4.51 mM; thus, K_d^{app} larger than 4.51 mM indicates internal binding in the distal pocket. The K_d^{app} values of the "native" substrate 2,4,6-TBP and inhibitor 4-BP phenol provide reference values for evaluation of other the internally bound molecules.

DOI: 10.1021/jp512996v
J. Phys. Chem. B XXXX, XXX, XXX−XXX

On the basis of this interpretation, the molecule 2,4-dibromophenol (2,4-DBP) has the tightest binding affinity of any molecule tested. It is therefore also the tightest binding among the three bromophenol substrates, 2,4,6-TBP, 2,4-DBP, and 4-BP. Its binding affinity is approximately 14-fold of that of 4-BP. To further probe the impact of the halogen substituted position on the aromatic ring, we have measured the K_d^{app} for 2-BP, 3-BP, and 2,6-DBP. 2-BP has shown larger K_d^{app} than 4-BP, which indicates that the ortho-position of the phenolic group may give a tighter binding affinity than the para-position. Unlike 4-BP, the binding of 2-BP to DHP gives rise to a charge transfer band at 636 nm and the Soret band is less blue-shifted compared to that of 4-BP. However, if both ortho-positions are occupied as in 2,6-dibromophenol (2,6-DBP), the binding affinity becomes dramatically lower. It is worth noting that 2,6-DBP has a lower binding affinity than 2,4,6-TBP. The contrast between 2,4-DBP and 2,6-DBP is striking. The former binds more tightly than 2,4,6-TBP by a factor of ~7, while the latter binds ~4 times more weakly. Unlike both 2-BP and 4-BP, 3-BP directly coordinates to the heme iron with the binding affinity K_d = 184.1 ± 8.6 μM that is 25-fold smaller than that of fluoride. The UV−vis spectrum of 3-BP DHP binding complex has the Soret band at 406 nm and a charge transfer band at 613 nm, which is quite distinct from the spectra for 2-BP and 4-BP binding (Figure S2).

Using the same strategy, we have measured the K_d^{app} of phenol, several substituted phenols, and three aromatic amino acids. As for most internal binding molecules, their dissociation constant K_L is usually much smaller than their concentration [L], especially when [L] = 5 mM. Thus, K_L can be ignored compared to [L]. Therefore, we can simplify eq 2 to show that K_L is inversely proportional to the K_d^{app}. On the basis of the K_d^{app} value, we conclude that phenol, *p*-cresol, guaiacol, 2,3,6-trimethylphenol, benzohydroxamic acid, and ferulic acid present moderate binding affinity toward DHP, which is about half of the binding affinity of the inhibitor 4-BP. The amino acids L-phenylalanine and L-tryptophan bind poorly and are estimated to possess only one-fifth binding affinity of 4-BP. In contrast, L-tyrosine shows binding affinity comparable to the 4-halogenated phenols.

Indole derivatives comprise a new class of substrate discovered along with the peroxygenase function of DHP.[3] Therefore, indole and its derivatives were also tested in competitive binding studies with fluoride to measure the corresponding K_d^{app} values. The 5-halogenated indole series (F, Cl, Br, I) clearly show a trend that the corresponding K_d^{app} increases as the radius of the halogen atom increases, which is consistent with previously reported binding affinity of 5-halogenated indoles. Moreover, the 5-position of the indole is most crucial in determining the indole derivative's binding affinity toward DHP because K_d^{app} of 5-bromoindole is approximately 2-fold higher than that for the 4-, 6-, and 7-bromoindoles. All of these relative binding affinities reported by K_d^{app} of fluoride titration are consistent with previous published resonance Raman spectra of indole derivatives of DHP B, in which ν_2 and ν_3 vibrational modes referred as coordination state marker modes were monitored to tell the binding affinity of the indole derivatives.

pH-Dependent Fluoride Titration. In contrast to HRP, the fluoride binding affinity of DHP is relatively stable between pH 5.0 and pH 7.0.[35] The K_d^f of DHP A at pH 7.0 is only about 1.7-fold of K_d^f at pH 5.0. The large increase of K_d^f at pH 8.0 is because approximately 50% of the DHP A is ligated with hydroxide, which competes with the fluoride binding in the axial position.[36] However, some of the internal binding molecules with pK_a of the phenolic group between 5.0 and 7.0 are sensitive to the pH because the population of the protonated or deprotonated species is determined by pH exponentially. It is believed that only the charge neutral form of halogenated phenols can bind internally in DHP because of the highly hydrophobic environment in the distal pocket. Indeed, for 2,4,6-TCP with pK_a = 6.6, the increase of K_d^{app} at pH 6.0 compared to pH 7.0 implies that there are more 2,4,6-TCP bound internally because of the increase population of the charge neutral form at pH 6.0 (Table 3). In the contrast, 4-BP with pK_a = 9.3 does not show a significant pH-dependent effect on the value of K_d^{app} between pH 5.0 and pH 7.0. To sum up, this pH-dependent fluoride titration experiment proves that only the charge neutral form of the substrate binds internally in the highly hydrophobic distal pocket.

Table 3. Fluoride Dissociation Constants K_d^f and K_d^{app} in Different pH

		K_d^{app} (mM)	
pH	K_d^f (mM), DHP A WT	DHP A + 4-BP (1 mM)	DHP A + 2,4,6-TCP (1 mM)
pH 5.0	2.6 ± 0.1	13.4 ± 0.3	NA
pH 6.0	3.1 ± 0.2	12.1 ± 0.2	38.7 ± 1.4
pH 7.0	4.5 ± 0.1	12.3 ± 0.8	14.5 ± 0.8
pH 8.0	17.2 ± 1.1	NA	66.7 ± 10.9

DHP−F Adduct Revealed by Resonance Raman Spectroscopy. Resonance Raman spectroscopy was used to characterize the DHP−F adduct in both high and low frequency regions (Figures 3 and 4). Moreover, the DHP−F adduct is assigned by the strong ν_2 mode at 1565 cm^{-1}, which indicates the presence of a 6cHS ligation, in agreement with previous observations.[34] We observe that there are two ν_3 modes in DHP without fluoride bound (bottom spectrum in Figure 3). This is in agreement with previous observations and arises from the fact that ferric DHP A exists in an equilibrium of 5cHS and 6cHS.[34] Both 5cHS and 6cHS are present in the metaquo form as indicated by the ν_3 shift from 1564 to 1565 cm^{-1} (Figure 3). In the low frequency region, the iron fluoride stretching band was previously assigned at 462 cm^{-1} for 430 nm excitation.[34] It has been assigned at 461 cm^{-1} for 410 nm

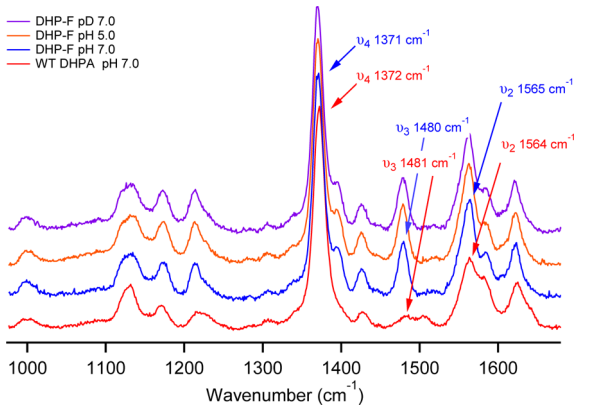

Figure 3. Resonance Raman spectra of WT ferric DHP A at pH 7.0 (red), DHP−F at pH 7.0 (blue), DHP−F at pH 5.0 (orange), and DHP−F at pD 7.0 (purple), in the high frequency region.

DOI: 10.1021/jp512996v
J. Phys. Chem. B XXXX, XXX, XXX−XXX

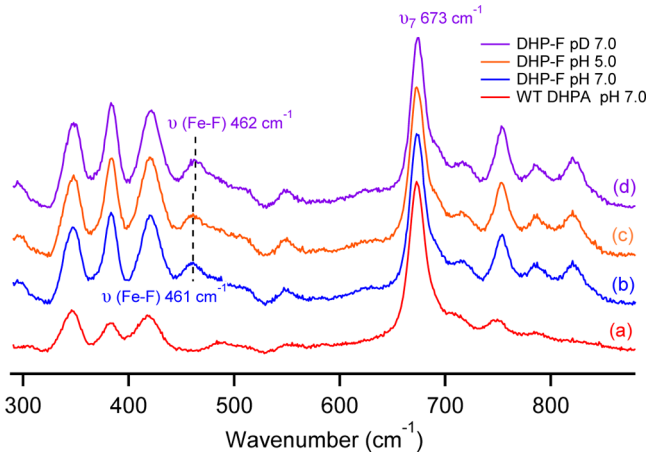

Figure 4. Resonance Raman spectra of WT ferric DHP A at pH 7.0 (red), DHP−F at pH 7.0 (blue), DHP−F at pH 5.0 (orange), and DHP−F at pD 7.0 (purple), in the low frequency region.

excitation in this study. The change of pH has no significant effect on the low frequency region in the resonance Raman spectra, which is reasonable because the binding affinity of fluoride is only enhanced by 1.7-fold when pH is shifted from 7.0 to 5.0. However, the Fe−F stretching band was shifted to 462 cm^{-1} in the KP_i buffer with D_2O at pD 7.0. The increased wavenumber of Fe−F stretching frequency indicates the enhancement of the Fe−F bond strength. One possible scenario is that there is a water molecule in the distal pocket that H-bonded to the fluoride anion. Replacement of H_2O with D_2O molecule will weaken the H-bond between water and fluoride, which in turn will enhance the Fe−F bond strength, resulting in a higher stretching frequency.

In Figure 5, upon the titration of the tightest binding substrate 2,4-DBP, we were able to observe the gradual

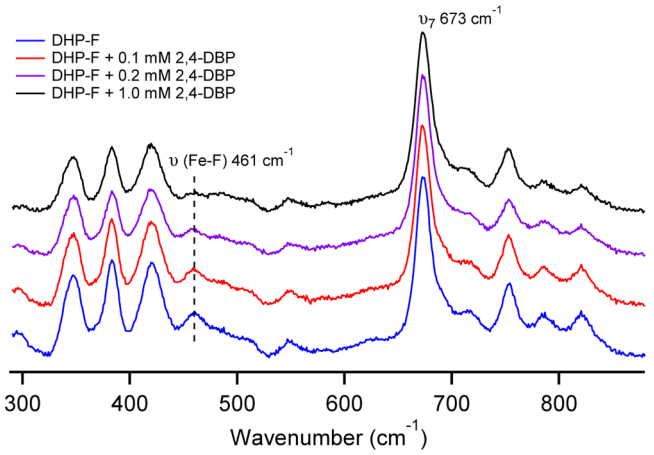

Figure 5. Resonance Raman spectra of DHP−F titrated with 0 mM 2,4-DBP (blue), 0.1 mM 2,4-DBP (red), 0.2 mM 2,4-DBP (purple), and 1.0 mM 2,4-DBP (black), in the low frequency region.

diminishing of the Fe−F stretching band at 461 cm^{-1} as the substrate concentration is increased. This clearly shows the fluoride ligand starting to dissociate upon the binding of 2,4-DBP, which indicates the strong competitive binding between fluoride anion and internal binding molecule. If there were any simultaneous binding, we would expect the intensity of the Fe−F stretch to be preserved and the frequency to be shifted. The comparison of pH and pD shows the kind of shift that can be expected.

Fe−F Bonding Studied by Density Functional Theory. DFT calculations were carried out on the heme models shown in Figure 6 and several other related models, which are

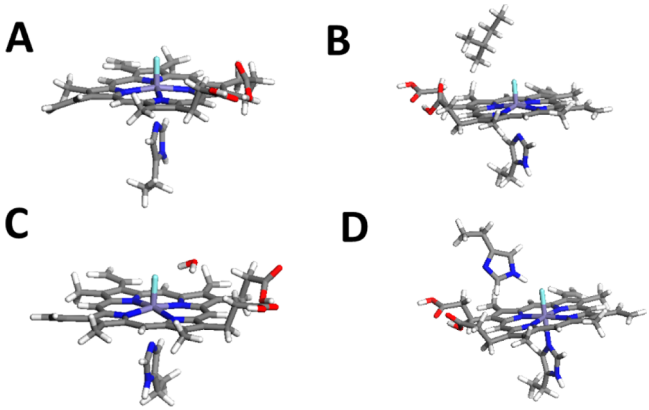

Figure 6. Stick figures of one of the series of structures used for model DFT calculations. The models shown are (A) proximal-His-heme-F, (B) proximal-His-heme-F-(Ile), (C) proximal-His-heme-F-(H_2O), and (D) proximal-His-heme-F-(His).

Table 4. Wave Number of the Fe−F Stretching Mode Calculated Using DFT Methods[a]

model		
proximal	distal	ν(Fe−F) (cm^{-1})
NA	NA	593
His	NA	550
His	His (NδH)	452
His	His (CH)	435
His	Ile	543
His	H_2O	496
His (H_2O)	NA	470
His (H_2O)	H_2O	489
His (H_2O)	His (NδH)	372
His (OH−)	NA	451

[a]All structures contained heme and fluoride with various groups on the proximal and distal side as given in columns 1 and 2.

described in Tables 4 and 5 in terms of the distal and proximal ligands. The vibrational frequencies and fluoride binding energies given in Tables 4 and 5, respectively, show that the strength of the Fe−F bond depends on both H-bonding (cis effect) and axial ligation (trans effect). Table 4 shows a general trend for the wavenumber of the Fe−F stretching mode in cm^{-1} to decrease with the strength of distal H-bonding. The trans effect produces an decrease in binding energy and wavenumber in direct proportion to the strength of the proximal interaction. The stronger is the trans ligation (i.e., for a more basic proximal ligand), the weaker is the Fe−F bond. Thus, for example, the strongest binding and highest frequency are observed for five-coordinate heme−F, the binding energy and ν(Fe−F) cm^{-1} decreasing in the order OH^-(His) < H_2O(His) < His < no ligand. The calculated F^--binding energies shown in Table 5 depend on both the distal H-bonding effect and the proximal trans ligation effect. Because of

DOI: 10.1021/jp512996v
J. Phys. Chem. B XXXX, XXX, XXX−XXX

Table 5. Solution and Binding Energies Calculated Using DFT Methods Including a COSMO Dielectric Continuum Model

heme species, proximal/distal	heme−F⁻, E (Ha)	heme, E (Ha)	ΔE (Ha)[a]	ΔE(F⁻ bind) (kcal/mol)[b]	ΔE(F⁻(aq)) (kcal/mol)[c]
NA/NA	−3196.85	−3096.83	−100.021	−24.4	−13.6
His/NA	−3501.47	−3401.47	−100.003	−18.8	−8.1
His/His (Nδ H)	−3806.08	−3706.07	−100.013	−21.9	−11.1
His/His (CH)	−3806.08	−3706.09	−99.995	−16.5	−5.7
His/Ile	−3699.02	−3599.02	−100.001	−18.4	−7.6
His/H_2O	−3577.86	−3477.87	−99.992	−15.5	−4.7
His(H_2O)/NA	−3577.86	−3477.85	−100.010	−21.1	−10.4
His(H_2O)/His (Nε H)	−3882.48	−3782.48	−100.004	−19.2	−8.5
His(H_2O)/H_2O	−3654.26	−3554.26	−100.008	−20.6	−9.8
His(OH^-)/NA	−3577.37	−3477.38	−99.986	−13.5	−2.7
His(OH^-)/His (Nε H)	−3881.99	−3781.99	−99.998	−17.4	−6.6

[a]This value is obtained by subtraction of column 2 from column 1. [b]The total energy of the F⁻ ion is −99.9429 Ha using the continuum dielectric model in H_2O (ε = 78.4). This value was added to ΔE in column to obtain F⁻ binding energy in the continuum model. [c]By use of this method, the solvation energy of F⁻ ion in a solvent model consisting of 16 H_2O molecules is −10.8 kcal/mol. The value in aqueous solution is obtained by subtracting the solvation energy of F⁻ ion in water (modeled as 16 H_2O molecules) from column 4.

the opposing distal and proximal trends, we must consider the distal and proximal effects separately. In comparison with the calculated binding energies on the proximal side, the H_2O(His) calculated binding energy does not follow the trend, but the other binding energies do follow the trend that increased axial (trans) ligation strength weakens the Fe−F bond. At the present time we have no explanation for the H_2O(His) anomaly. Distal ligation binding energies are complicated by the fact that there are two contributions to the binding energy. The introduction of H-bonding on the distal side weakens the Fe−F bonding interaction. However, the total binding energy of F⁻ must also take the hydrogen binding interaction of Fe−H into account. This fact prohibits direct comparison of these binding energies with the Fe−F frequencies, for example, since the frequencies report only on the force constant of the Fe−F bond.

The DFT calculations show that the cis effect of distal histidine His or a distal water molecule significantly lowers the Fe−F stretching frequency by a H-bonding interaction, which is consistent with previously observed shifted ν(Fe−F) stretching frequency in the series of mutated Tf-trHb by resonance Raman spectroscopy.[37] It is relevant that DHP has an observed ν(Fe−F) stretch of 461 cm^{-1}, which is in the correct range for a model with both a proximal histidine and moderately strong H-bonding by a distal histidine. The calculated wavenumber was not scaled or corrected for anharmonicity. The trends on the distal side agree with the general idea that hydrophobic amino acids in the distal position have weak H-bonding (e.g., Ile in Table 4), and therefore the ν(Fe−F) stretching frequency increases.

DISCUSSION

On the Choice of Fluoride as the Ligand for a Competitive Binding Assay. Structural methods can provide information about the modes of binding of substrates and inhibitors, but they require a great deal of time and effort. The current study is not a substitute for structural studies but a competitive binding assay that is relatively easy to implement, since UV−vis spectroscopy can be used to detect the displacement of ligands bound to the heme Fe. We have already reported such an assay, in which the naturally occurring H_2O ligand is displaced by inhibitor binding.[7,34] However, the H_2O competition assay is of limited utility because the shifts in the resonance Raman spectrum are quite small. The drawback of using H_2O ligand as a probe is that there is only about 60% of the metaquo form at pH 6.0.[38] It is difficult to monitor the change of the coordination state in the UV−vis because there is no significant shift in the Soret, Q-band, or charge-transfer band regions of the spectrum, but the structural conclusions have been corroborated by the use of electron paramagnetic resonance.[39,40] CO is a diatomic probe that can also be used based on the Fe−C stretching band of the CO adduct monitored using resonance Raman spectroscopy between 400−600 cm^{-1} and the C−O vibrational mode observed by IR spectroscopy.[41−43] However, CO only binds to the ferrous form of the heme, which is not the typical oxidation state for the starting point of peroxidase or peroxygenase chemistry. Moreover, CO binding is quite strong and there is no evidence for any competition with substrate binding.[36,44] Fluoride binding provides similar information to CO in that laser excitation in the Soret band region can give significant enhancement of the Fe−F stretching band at 461 cm^{-1} in the resonance Raman spectrum, which also provides a probe of internal large molecule binding.[42,45] Fluoride has moderate binding affinity to the heme Fe so that two modes of interaction can be studied. Competitive binding will lead to loss of the Fe−F intensity. Simultaneous binding will lead to a shift in the Fe−F stretching frequency. Finally, the titration experiments can be carried out with no need for an anaerobic environment as required for CO adducts.

On the Competition between Noncovalent Substrate and Covalent Fluoride Binding. The competitive binding assay is based on the observation that a noncovalent internal substrate/inhibitor binding has an energy comparable to the bond ligation energy of fluoride. Using the K_d^f values Table 1, we can estimate the binding free energy of fluoride. Using $\Delta G^\circ = -RT \ln(K_a)$ for the binding energy. Since $K_a = 1/K_d^f \approx 220$ M^{-1}, we can estimate the free energy as approximately −3.2 kcal/mol. Since the substrates/inhibitors can displace fluoride in same concentration range, their binding energies must be comparable to the covalent binding of fluoride itself. Of course, the competitive binding by mass action is concentration dependent. The calculated free energies from the Fe−F bond are comparable to the experimental range. The various models attempt to capture the possible range of distal and proximal effects in heme proteins with calculated binding energies ranging from −2.7 to −11.1 kcal/mol.

DOI: 10.1021/jp512996v
J. Phys. Chem. B XXXX, XXX, XXX−XXX

The computational model in Table 5 suggests that if the H-bond with His[55] is disrupted, which occurs when the inhibitor 4-BP binds in the distal pocket, the binding energy of fluoride should increase by +3.0 kcal/mol. This value is obtained by comparing the model with a distal histidine that can H-bond (NδH) and no ligand on the distal side (NA) in rows 3 and 2, respectively, of Table 5. The same comparison when a water molecule is on the proximal side H-bonded to the proximal histidine gives +3.4 kcal/mol in rows 5 and 2, respectively, of Table 5. This is the value that is relevant to the binding of substrate. The experimental binding energy of approximately −3.2 kcal/mol is consistent with the observation that the internal substrate (or inhibitor) binding can displace F^-. We can identify the distal H-bonding as the main cause of the destabilization of F^-. This conclusion is consistent with a large body of work on binding F^- in heme proteins and its use as a probe of the distal environment. The COSMO calculation gives a range values, which are comparable to the experimental value of −3.2 kcal/mol. Since this value is at low end of the range in Table 5, the most appropriate model may be one in which the proximal histidine is partially polarized His(OH^-), which has been suggested based on resonance Raman data and DFT calculations.[41,46,47] Calculation of the hydration energy

$$16H_2O + F^- \rightarrow 16H_2O{:}F^-$$

using DFT methods gives −10.8 kcal/mol, which is in the range of possible values given in Table S1, which is taken from the CRC Handbook. Both the absolute and relative binding strengths obtained from DFT calculations are in the correct ranges and agree with experimental trends.

Role of Distal Histidine His[55] in H-Bond Interactions of DHP−F Adduct. The DHP−F adduct has a characteristic charge transfer band at 605 nm that can be observed in the UV−vis spectrum. This charge transfer band CT1 is due to the $[a_{2u}(\pi) \rightarrow e_g(d_\pi)]$ transition from porphyrin ring to heme iron.[48] The CT1 band of DHP is relatively blue-shifted compared to the CT1 band of other hemoproteins (SWMb, hhMb, HRP, and CcP) fluoride adduct, which indicates that there are fewer H-bonding interactions in the distal pocket to stabilize the fluoride anion. Similar to SWMb, the distal histidine is the only residue that is responsible for stabilizing the fluoride anion in DHP. Evidence for the stabilization of fluoride by distal histidine H-bonding is found in the DHP A H55D mutant, which completely loses the ability to bind fluoride anion. Similar observations have been made for SWMb H64V and H64L mutants.[49] The corresponding H55V mutant in DHP A is completely nonfunctional, consistent with the role played by the distal histidine in stabilization of ligand binding at the heme Fe.[50] However, the CT1 band of DHP−F is observed at 605 nm over the pH range 5.0−7.0, concomitant with the lack of change in the Fe−F stretching band at 461 cm^{-1} at both pH 5.0 and pH 7.0. This behavior is in contrast to HHMb, which has two pH-dependent forms of fluoride-bound complex.[48] This observation is consistent with the hypothesis that the pH dependence of reactivity DHP A is due to the ionization of the substrate rather than an effect of pH on the protein.[22,24,51] The stabilization of bound fluoride by a "heme-linked" amino acid, which is most likely the distal histidine, has been observed using fluoride binding kinetics in HRP.[35] The idea of using fluoride as a probe has been exploited in many studies of peroxidases using UV−vis and resonance Raman spectroscopy.[17,52−55]

The distal pocket of DHP must possess flexibility to accommodate such a wide range of molecules in the distal pocket. Besides the allosteric distal histidine His[55], hydrophobic residues Phe[21], Phe[35], and Val[59] should stabilize the internal binding molecules through van de Waals interaction.[7,10,38,44] A series of X-ray crystal structures, NMR studies, and resonance Raman studies have shown that H55 is unusually flexible in DHP when compared to the distal histidine of other globins.[7,56] The flexibility appears to be important in the competitive fluoride binding studies as well. The distal histidine, H55, is essential for stabilizing the fluoride binding in DHP. It is known that the distal histidine is the residue that fine-tunes exogenous ligand binding in myoglobin. DHP has a similar scenario because the distal histidine, H55, is the only polar residue in the distal pocket. Such a role for the distal histidine has already been established based on strong H-bond to the dioxygen ligand in the oxyferrous form and H-bonding to H_2O in the metaquo form.[38] However, the DHP-CO turns out to be an exception as the distal histidine H55 is observed mostly adopting solvent exposed "open" conformation because of the weak H-bond interactions between H55 and heme-bound CO but rather strong H-bonds interaction between H55 and the propionates.[57] The greater flexibility of the distal histidine in DHP relative to other globins suggests that there could be stronger H-bonding in DHP. One possible scenario is that distal histidine H55 mediates an indirect H-bonding to fluoride anion through a water molecule in the distal pocket (Scheme 2). This scenario is possible because a water molecule can

Scheme 2. Proposed H-Bonding Interactions with Fluoride in DHP

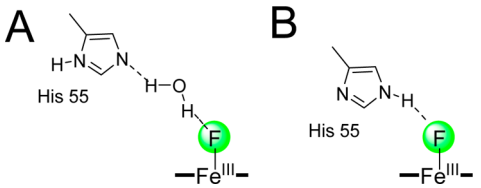

reside in the distal pocket as observed in the X-ray crystallographic structures of PDB code 1EW6 at room temperature and PDB code 2QFK at 100 K. For an intermediate H_2O molecule to be present as shown in Scheme 2A, His[55] would need to be present in the NδH tautomer. The isotope effect in this model would be explained by replacement of H_2O by D_2O. Another scenario is that distal histidine directly interacts with fluoride where the H-bond is NεH···F. In this case shown in Scheme 2B, the H-bonding would be weakened in D_2O solution by H/D exchange, NεH(D)···F. In the case of SWMb, the fluoride is H-bonded to the distal histidine, H64, and a solvent water molecule that significantly interacts with the same distal histidine.[49] The Fe−F stretching band in DHP is 1 cm^{-1} higher in D_2O than that in H_2O and indicates that the strength of Fe−F bond is enhanced because of the weakened H-bonding. This conclusion is also consistent with the DFT calculations given in Table 4. However, we do not have sufficient information at this time to decide between the two models in Scheme 2.

Natural Selection and Selective Internal Binding of Molecules in the Distal Pocket. The current results show that DHP is promiscuous with regard substrate binding, which is similar to the xenobiotic metabolizing cytochrome P450 enzymes.[58] However, the trend of binding affinity between

DOI: 10.1021/jp512996v
J. Phys. Chem. B XXXX, XXX, XXX−XXX

brominated phenols (2,4-DBP > 2,4,6-TBP > 4-BP) still presents some selectivity toward these substrates which may be a result of evolution.[59,60] *Amphitrite ornata* cohabitates with another polychaete marine worm *Notomastus lobatus*, a subsurface filter feeder that secrets halogenated phenols to repel potential predators.[5] Since *A. ornata* itself does not possess this "chemical weapon", it appears that the most abundant protein in *A. ornata*, DHP, has evolved a peroxidase function as a natural protection against the toxicity of brominated compounds. Chemical analyses of volatile organohalogen compounds show that *N. lobatus* contains abundant amount of 2,4-DBP and moderate amount of 2,4,6-TBP and 4-BP. Thus, 2,4-DBP may be the primary substrate of DHP in nature. The structural evidence suggests that 2,4-DBP is adapted to the substrate binding site observed in the 2,4,6-TBP X-ray crystal structure.[8] First, 2,4-DBP also functions as a substrate in the presence of H_2O_2 (Figure S1). Moreover, the ortho-bromo substituents make the 2,4-DBP unlikely to bind in the inhibitor binding site because of steric hindrance. While 2,6-DBP has not been identified in *N. lobatus*, it has been observed in another polychaete lugworm, *Arenicola brasiliensis*, that is also a subsurface filter feeder.[59] The ratio of the binding constants for the various brominated phenols studied in this work matches the abundance of brominated phenols in the benthic ecosystem where *A.ornata* lives. Therefore, it is reasonable to postulate that natural selection may play a role in shaping the internal binding site of DHP.

While bromoindoles are much less prevalent in benthic ecosystems, the binding of indoles in the distal pocket of a heme protein is similar to the binding of substrates in the mammalian enzymes, indoleamine 2,3-dioxygenase and tryptophan dioxygenase. The determinants of substrate binding in these proteins have been probed in molecule detail using site-directed mutagenesis,[61] following similar detailed studies in peroxidases.[62] These observations are relevant for this study, since spectroscopy has been used to quantify this binding in the dioxygenases.[63] Moreover, substrate inhibition is a recurrent theme in these studies of dioxygenases, as is observed in DHP as well.[13,64]

CONCLUSION

The present study permits a comparison of substrates and inhibitors that have different modes of binding. Both substrates and inhibitors bind in the distal pocket of the DHP protein in sites we call the α- and β-sites in Figure 1. From previous structural work it was known that 4-halogenated phenols (except 4-FP) act as inhibitors of DHP and bind in a well-defined binding site. One of the principal determinants of binding in the β-site is the presence of a Xe binding site in DHP, which is where the halogen of 4-BP resides when it is bound in the β-site.[65] The hypothesized peroxygenase substrates 2,4-DCP and 2,4-DBP are suspected to bind in a substrate binding site at the α-heme edge. This alternative internal binding site is deep inside the protein.[8,9] The known peroxidase substrates, 2,4,6-TCP and 2,4,6-TBP, are believed to bind at an external site near the heme δ-edge at low concentration, but they are also observed to bind at the heme α-edge internal site at higher concentration.[8,9] The relative binding strengths of these large molecules are consistent with a functional interpretation of the two major internal modes of binding shown in Figure 1. The nearly perpendicular binding of the β-site very near the heme Fe makes it an inhibitor, since it blocks the heme Fe so H_2O_2 cannot bind and since it displaces the distal histidine (H55) so that it cannot act as an acid−base catalyst in the peroxidase function. The α-site places the substrate in an orientation that permits H-bonding by the phenolic O−H to a bound ligand (e.g., H_2O_2), and it exposes the C−H in the 6-position so that it is poised for oxygen atom transfer in the peroxygenase function. This study shows that 2,4-DBP binds more tightly in the protein than any other ligand, which presumably means that it binds in the α-site. The data show that although 2,4,6-TBP also binds the in α-site, its binding is much weaker. While 2,4,6-TBP cannot compete with 2,4-DBP, it is capable of autoinhibition or substrate inhibition at high 2,4,6-TBP concentration. These trends, apparent in the study using a competitive fluoride binding assay, provide a consistent picture of the relative strength of binding interactions needed to permit three of the protein functions of DHP to coexist; the globin, peroxidase, and peroxygenase functions. It also explains the relative magnitude of inhibition for 4-BP. These provide important relative binding strengths for the bromoindoles, which will contribute to our understanding as further mechanistic studies on the peroxygenase and oxidase functions of DHP emerge.

ASSOCIATED CONTENT

Supporting Information

Derivation of the apparent binding equilibrium constant, UV−vis spectra, and heat of fluoride solution. This material is available free of charge via the Internet at http://pubs.acs.org.

AUTHOR INFORMATION

Corresponding Author

*E-mail: franzen@ncsu.edu.

Notes

The authors declare no competing financial interest.

ACKNOWLEDGMENTS

This work was supported by Army Research Office Grant 57861-LS.

REFERENCES

(1) Weber, R. E.; Mangum, C.; Steinman, H.; Bonaventura, C.; Sullivan, B.; Bonaventura, J. Hemoglobins of Two Terebellid Polychaetes: *Enoplobranchus sanguineus* and *Amphitrite ornata*. *Comp. Biochem. Physiol., Part A: Physiol.* **1977**, *56* (2), 179−187.

(2) Franzen, S.; Thompson, M. K.; Ghiladi, R. A. The Dehaloperoxidase Paradox. *Biochim. Biophys. Acta, Proteins Proteomics* **2012**, *1824*, 578−588.

(3) Barrios, D. A.; D'Antonio, J.; McCombs, N. L.; Zhao, J.; Franzen, S.; Schmidt, A. C.; Sombers, L. A.; Ghiladi, R. A. Peroxygenase and Oxidase Activities of Dehaloperoxidase-Hemoglobin from *Amphitrite ornata*. *J. Am. Chem. Soc.* **2014**, *136* (22), 7914−7925.

(4) Du, J.; Huang, X.; Sun, S. F.; Wang, C. X.; Lebioda, L.; Dawson, J. H. *Amphitrite ornata* Dehaloperoxidase (DHP): Investigations of Structural Factors That Influence the Mechanism of Halophenol Dehalogenation Using "Peroxidase-like" Myoglobin Mutants and :Myoglobin-like" DHP Mutants. *Biochemistry* **2011**, *50* (38), 8172−8180.

(5) Chen, Y. P.; Woodin, S. A.; Lincoln, D. E.; Lovell, C. R. An Unusual Dehalogenating Peroxidase from the Marine Terebellid Polychaete *Amphitrite ornata*. *J. Biol. Chem.* **1996**, *271* (9), 4609−4612.

(6) D'Antonio, J.; Ghiladi, R. A. Reactivity of Deoxy- and Oxyferrous Dehaloperoxidase B from *Amphitrite ornata*: Identification of Compound II and Its Ferrous-Hydroperoxide Precursor. *Biochemistry* **2011**, *50* (27), 5999−6011.

DOI: 10.1021/jp512996v
J. Phys. Chem. B XXXX, XXX, XXX−XXX

(7) Thompson, M. K.; Davis, M. F.; de Serrano, V.; Nicoletti, F. P.; Howes, B. D.; Smulevich, G.; Franzen, S. Internal Binding of Halogenated Phenols in Dehaloperoxidase-Hemoglobin Inhibits Peroxidase Function. *Biophys. J.* **2010**, *99* (5), 1586−1595.
(8) Zhao, J.; Zhao, J.; Franzen, S. The Regulatory Implications of Hydroquinone for the Multifunctional Enzyme Dehaloperoxidase-Hemoglobin from *Amphitrite ornata*. *J. Phys. Chem. B* **2013**, *117* (47), 14615−14624.
(9) Wang, C.; Lovelace, L. L.; Sun, S.; Dawson, J. H.; Lebioda, L. Complexes of Dual-Function Hemoglobin/Dehaloperoxidase with Substrate 2,4,6-Trichlorophenol Are Inhibitory and Indicate Binding of Halophenol to Compound I. *Biochemistry* **2013**, *52* (36), 6203−6210.
(10) Davis, M. F.; Gracz, H.; Vendeix, F. A. P.; de Serrano, V.; Somasundaram, A.; Decatur, S. M.; Franzen, S. Different Modes of Binding of Mono-, Di-, and Trihalogenated Phenols to the Hemoglobin Dehaloperoxidase from *Amphitrite ornata*. *Biochemistry* **2009**, *48* (10), 2164−2172.
(11) Davis, M. F.; Bobay, B. G.; Franzen, S. Determination of Separate Inhibitor and Substrate Binding Sites in the Dehaloperoxidase-Hemoglobin from Amphitrite ornata. *Biochemistry* **2010**, *49* (6), 1199−1206.
(12) Du, J.; Sono, M.; Dawson, J. H. Functional Switching of *Amphitrite ornata* Dehaloperoxidase from O_2-Binding Globin to Peroxidase Enzyme Facilitated by Halophenol Substrate and H_2O_2. *Biochemistry* **2010**, *49* (29), 6064−6069.
(13) Lu, C. Y.; Lin, Y.; Yeh, S. R. Inhibitory Substrate Binding Site of Human Indoleamine 2,3-Dioxygenase. *J. Am. Chem. Soc.* **2009**, *131* (36), 12866−12867.
(14) Kuo, H. H.; Mauk, A. G. Indole Peroxygenase Activity of Indoleamine 2,3-Dioxygenase. *Proc. Natl. Acad. Sci. U.S.A.* **2012**, *109* (35), 13966−13971.
(15) Sturgeon, B. E.; Battenburg, B. J.; Lyon, B. J.; Franzen, S. Revisiting the Peroxidase Oxidation of 2,4,6-Trihalophenols: ESR Detection of Radical Intermediates. *Chem. Res. Toxicol.* **2011**, *24* (11), 1862−1868.
(16) Franzen, S.; Sasan, K.; Sturgeon, B. E.; Lyon, B. J.; Battenburg, B. J.; Gracz, H.; Dumariah, R.; Ghiladi, R. Nonphotochemical Base-Catalyzed Hydroxylation of 2,6-Dichloroquinone by H_2O_2 Occurs by a Radical Mechanism. *J. Phys. Chem. B* **2012**, *116* (5), 1666−1676.
(17) Neri, F.; Kok, D.; Miller, M. A.; Smulevich, G. Fluoride Binding in Hemoproteins: The Importance of the Distal Cavity Structure. *Biochemistry* **1997**, *36* (29), 8947−8953.
(18) Lebioda, L.; LaCount, M. W.; Zhang, E.; Chen, Y. P.; Han, K.; WHitton, M. M.; Lincoln, D. E.; Woodin, S. A. An Enzymatic Globin from a Marine Worm. *Nature* **1999**, *401*, 445.
(19) Smulevich, G.; Feis, A.; Howes, B. D. Fifteen Years of Raman Spectroscopy of Engineered Heme Containing Peroxidases: What Have We Learned? *Acc. Chem. Res.* **2005**, *38* (5), 433−440.
(20) D'Antonio, J.; D'Antonio, E. L.; Thompson, M. K.; Bowden, E. F.; Franzen, S.; Smirnova, T.; Ghiladi, R. A. Spectroscopic and Mechanistic Investigations of Dehaloperoxidase B from *Amphitrite ornata*. *Biochemistry* **2010**, *49* (31), 6600−6616.
(21) de Serrano, V.; D'Antonio, J.; Franzen, S.; Ghiladi, R. A. Crystal Structure of Dehaloperoxidase B at 1.58 Å and Characterization of the A/B Dimer from *Amphitrite ornata*. *Acta. Crystallogr. D* **2010**, *66*, 529−538.
(22) Schkolnik, G.; Salewski, J.; Millo, D.; Zebger, I.; Franzen, S.; Hildebrandt, P. Vibrational Stark Effect of the Electric-Field Reporter 4-Mercaptobenzonitrile as a Tool for Investigating Electrostatics at Electrode/SAM/Solution Interfaces. *Int. J. Mol. Sci.* **2012**, *13* (6), 7466−7482.
(23) Zhao, J. J.; Rowe, J.; Franzen, J.; He, C.; Franzen, S. Study of the Electrostatic Effects of Mutations on the Surface of Dehaloperoxidase-Hemoglobin A. *Biochem. Biophys. Res. Commun.* **2012**, *420* (4), 733−737.
(24) Schkolnik, G.; Utesch, T.; Zhao, J.; Jiang, S.; Thompson, M. K.; Mroginski, M. A.; Hildebrandt, P.; Franzen, S. Catalytic Efficiency of Dehaloperoxidase A Is Controlled by Electrostatics—Application of the Vibrational Stark Effect To Understand Enzyme Kinetics. *Biochem. Biophys. Res. Commun.* **2013**, *430* (3), 1011−1015.
(25) Zhao, J.; de Serrano, V.; Dumarieh, R.; Thompson, M.; Ghiladi, R. A.; Franzen, S. The Role of the Distal Histidine in H_2O_2 Activation and Heme Protection in Both Peroxidase and Globin Functions. *J. Phys. Chem. B* **2012**, *116* (40), 12065−12077.
(26) Ma, H.; Thompson, M. K.; Gaff, J.; Franzen, S. Kinetic Analysis of a Naturally Occurring Bioremediation Enzyme: Dehaloperoxidase-Hemoglobin from *Amphitrite ornata*. *J. Phys. Chem. B* **2010**, *114* (43), 13823−13829.
(27) Osborne, R. L.; Taylor, L. O.; Han, K. P.; Ely, B.; Dawson, J. H. *Amphitrite ornata* Dehaloperoxidase: Enhanced Activity for the Catalytically Active Globin Using MCPBA. *Biochem. Biophys. Res. Commun.* **2004**, *324* (4), 1194−1198.
(28) Berry, E. A.; Trumpower, B. L. Simultaneous Determination of Hemes *a*, *b*, and *c* from Pyridine Hemochrome Spectra. *Anal. Biochem.* **1987**, *161* (1), 1−15.
(29) Delley, B. From Molecules to Solids with the DMol3 Approach. *J. Chem. Phys.* **2000**, *113* (18), 7756−7764.
(30) Delley, B. An All-Electron Numerical Method for Solving the Local Density Functional for Polyatomic Molecules. *J. Chem. Phys.* **1990**, *92* (1), 508−517.
(31) Perdew, J. P.; Burke, K.; Wang, Y. Generalized Gradient Approximation for the Exchange-Correlation Hole of a Many-Electron System. *Phys. Rev. B* **1996**, *54* (23), 16533−16539.
(32) Klamt, A.; Schuurmann, G. COSMO: A New Approach to Dielectric Screening in Solvents with Explicit Expressions for the Screening Energy and Its Gradient. *J. Chem. Soc., Perkin Trans. 2* **1993**, No. 5, 799−805.
(33) Delley, B. Modern Density Functional Theory. In *Modern Density Functional Theory: A Tool for Chemistry*; Seminario, J. M., Politzer, P., Eds.; Theoretical and Computational Chemistry, Vol. 2; Elsevier: Amsterdam, 1995; p 221.
(34) Nicoletti, F. P.; Thompson, M. K.; Howes, B. D.; Franzen, S.; Smulevich, G. New Insights into the Role of Distal Histidine Flexibility in Ligand Stabilization of Dehaloperoxidase-Hemoglobin from *Amphitrite ornata*. *Biochemistry* **2010**, *49* (9), 1903−1912.
(35) Dunford, H. B.; Alberty, R. A. The Kinetics of Fluoride Binding by Ferric Horse Radish Peroxidase. *Biochemistry* **1967**, *6* (2), 447−451.
(36) Nienhaus, K.; Deng, P. C.; Belyea, J.; Franzen, S.; Nienhaus, G. U. Spectroscopic Study of Substrate Binding to the Carbonmonoxy Form of Dehaloperoxidase from *Amphitrite ornata*. *J. Phys. Chem. B* **2006**, *110* (26), 13264−13276.
(37) Nicoletti, F. P.; Droghetti, E.; Boechi, L.; Bonamore, A.; Sciamanna, N.; Estrin, D. A.; Feis, A.; Boffi, A.; Smulevich, G. Fluoride as a Probe for H-Bonding Interactions in the Active Site of Heme Proteins: The Case of *Thermobifida fusca* Hemoglobin. *J. Am. Chem. Soc.* **2011**, *133* (51), 20970−20980.
(38) de Serrano, V.; Chen, Z. X.; Davis, M. F.; Franzen, S. X-ray Crystal Structural Analysis of the Binding Site in the Ferric and Oxyferrous Forms of the Recombinant Heme Dehaloperoxidase Cloned from *Amphitrite ornata*. *Acta. Crystallogr. D* **2007**, *63*, 1094−1101.
(39) Smirnova, T. I.; Weber, R. T.; Davis, M. F.; Franzen, S. Substrate Binding Triggers a Switch in the Iron Coordination in Dehaloperoxidase from *Amphitrite ornata*: HYSCORE experiments. *J. Am. Chem. Soc.* **2008**, *130* (7), 2128−2129.
(40) Thompson, M. K.; Franzen, S.; Ghiladi, R. A.; Reeder, B. J.; Svistunenko, D. A. Compound ES of Dehaloperoxidase Decays via Two Alternative Pathways Depending on the Conformation of the Distal Histidine. *J. Am. Chem. Soc.* **2010**, *132* (49), 17501−17510.
(41) Franzen, S.; Roach, M. P.; Chen, Y.-P.; Dyer, R. B.; Woodruff, W. H.; Dawson, J. H. The Unusual Reactivities of *Amphitrite ornata* Dehaloperoxidase and *Notomastus lobatus* Chloroperoxidase Do Not Arise from a Histidine Imidazolate Proximal Heme Iron Ligand. *J. Am. Chem. Soc.* **1998**, *120* (19), 4658−4661.
(42) Spiro, T. G.; Soldatova, A. V.; Balakrishnan, G. CO, NO and O_2 as Vibrational Probes of Heme Protein Interactions. *Coord. Chem. Rev.* **2013**, *257* (2), 511−527.

DOI: 10.1021/jp512996v
J. Phys. Chem. B XXXX, XXX, XXX−XXX

(43) Mak, P. J.; Gregory, M. C.; Sligar, S. G.; Kincaid, J. R. Resonance Raman Spectroscopy Reveals That Substrate Structure Selectively Impacts the Heme-Bound Diatomic Ligands of CYP17. *Biochemistry* **2014**, *53* (1), 90−100.
(44) Nienhaus, K.; Nickel, E.; Davis, M. F.; Franzen, S.; Nienhaus, G. U. Determinants of Substrate Internalization in the Distal Pocket of Dehaloperoxidase Hemoglobin of *Amphitrite ornata*. *Biochemistry* **2008**, *47* (49), 12985−12994.
(45) Kitagawa, T.; Mizutani, Y. Resonance Raman-Spectra of Highly Oxidized Metalloporphyrins and Heme-Proteins. *Coord. Chem. Rev.* **1994**, *135*, 685−735.
(46) Franzen, S. Effect of a Charge Relay on the Vibrational Frequencies of Carbonmonoxy Iron Porphine Adducts: The Coupling of Changes in Axial Ligand Bond Strength and Porphine Core Size. *J. Am. Chem. Soc.* **2001**, *123* (50), 12578−12589.
(47) Franzen, S. An Electrostatic Model for the Frequency Shifts in the Carbonmonoxy Stretching Band of Myoglobin: Correlation of Hydrogen Bonding and the Stark Tuning Rate. *J. Am. Chem. Soc.* **2002**, *124* (44), 13271−13281.
(48) Droghetti, E.; Nicoletti, F. P.; Bonamore, A.; Sciamanna, N.; Boffi, A.; Feis, A.; Smulevich, G. The Optical Spectra of Fluoride Complexes Can Effectively Probe H-Bonding Interactions in the Distal Cavity of Heme Proteins. *J. Inorg. Biochem.* **2011**, *105* (10), 1338−1343.
(49) Aime, S.; Fasano, M.; Paoletti, S.; Cutruzzola, F.; Desideri, A.; Bolognesi, M.; Rizzi, M.; Ascenzi, P. Structural Determinants of Fluoride and Formate Binding to Hemoglobin and Myoglobin: Crystallographic and 1H-NMR Relaxometric Study. *Biophys. J.* **1996**, *70* (1), 482−488.
(50) Franzen, S.; Chaudhary, C.; Belyea, J.; Gilvey, L.; Davis, M. F.; Sit, T. L.; Lommel, S. A. Proximal Cavity, Distal Histidine and Substrate Hydrogen-Bonding Mutations Modulate the Activity of *Amphitrite ornata* Dehaloperoxidase. *Biochemistry* **2006**, *45*, 9085−9094.
(51) Franzen, S.; Gilvey, L. B.; Belyea, J. L. The pH Dependence of the Activity of Dehaloperoxidase from *Amphitrite ornata*. *Biochim. Biophys. Acta, Proteins Proteomics* **2007**, *1774* (1), 121−130.
(52) Howes, B. D.; Veitch, N. C.; Smith, A. T.; White, C. G.; Smulevich, G. Haem-Linked Interactions in Horseradish Peroxidase Revealed by Spectroscopic Analysis of the Phe-221 → Met Mutant. *Biochem. J.* **2001**, *353*, 181−191.
(53) Nissum, M.; Neri, F.; Mandelman, D.; Poulos, T. L.; Smulevich, G. Spectroscopic Characterization of Recombinant Pea Cytosolic Ascorbate Peroxidase: Similarities and Differences with Cytochrome *c* Peroxidase. *Biochemistry* **1998**, *37* (22), 8080−8087.
(54) Neri, F.; Indiani, C.; Baldi, B.; Vind, J.; Welinder, K. G.; Smulevich, G. Role of the Distal Phenylalanine 54 on the Structure, Stability, and Ligand Binding of Coprinus cinereus Peroxidase. *Biochemistry* **1999**, *38* (24), 7819−7827.
(55) Heering, H. A.; Jansen, M. A. K.; Thorneley, R. N. F.; Smulevich, G. Cationic Ascorbate Peroxidase Isoenzyme II from Tea: Structural Insights into the Heme Pocket of a Unique Hybrid Peroxidase. *Biochemistry* **2001**, *40* (34), 10360−10370.
(56) Chen, Z.; de Serrano, V.; Betts, L.; Franzen, S. Distal Histidine Conformational Flexibility in Dehaloperoxidase from *Amphitrite ornata*. *Acta. Crystallogr. D* **2009**, *65* (1), 34−40.
(57) Zhao, J.; de Serrano, V.; Franzen, S. A Model for the Flexibility of the Distal Histidine in Dehaloperoxidase-Hemoglobin A Based on X-ray Crystal Structures of the Carbon Monoxide Adduct. *Biochemistry* **2014**, *53* (15), 2474−2482.
(58) Poulos, T. L. Heme Enzyme Structure and Function. *Chem. Rev.* **2014**, *114* (7), 3919−3962.
(59) Fielman, K. T.; Woodin, S. A.; Walla, M. D.; Lincoln, D. E. Widespread Occurrence of Natural Halogenated Organics among Temperate Marine Infauna. *Mar. Ecol.: Prog. Ser.* **1999**, *181*, 1−12.
(60) Lincoln, D. E.; Fielman, K. T.; Marinelli, R. L.; Woodin, S. A. Bromophenol Accumulation and Sediment Contamination by the Marine Annelids *Notomastus lobatus* and *Thelepus crispus*. *Biochem. Syst. Ecol.* **2005**, *33*, 559−570.
(61) Chauhan, N.; Basran, J.; Rafice, S. A.; Efimov, I.; Millett, E. S.; Mowat, C. G.; Moody, P. C. E.; Handa, S.; Raven, E. L. How Is the Distal Pocket of a Heme Protein Optimized for Binding of Tryptophan? *FEBS. J.* **2012**, *279* (24), 4501−4509.
(62) Dunford, H. B. *Peroxidases and Catalases: Biochemistry, Biophysics, Biotechnology and Physiology*; John Wiley: Chichester, U.K., 2010.
(63) Lu, C. Y.; Lin, Y.; Yeh, S. R. Spectroscopic Studies of Ligand and Substrate Binding to Human Indoleamine 2,3-Dioxygenase. *Biochemistry* **2010**, *49* (24), 5028−5034.
(64) Efimov, I.; Basran, J.; Sun, X.; Chauhan, N.; Chapman, S. K.; Mowat, C. G.; Raven, E. L. The Mechanism of Substrate Inhibition in Human Indoleamine 2,3-Dioxygenase. *J. Am. Chem. Soc.* **2012**, *134* (6), 3034−3041.
(65) de Serrano, V.; Franzen, S. Structural Evidence for Stabilization of Inhibitor Binding by a Protein Cavity in the Dehaloperoxidase-Hemoglobin from *Amphitrite ornata*. *Biopolymers* **2012**, *98* (1), 27−35.
(66) Kosowicz, J. G.; Boon, E. M. Insights into the Distal Heme Pocket of H-NOX Using Fluoride as a Probe for H-Bonding Interactions. *J. Inorg. Biochem.* **2013**, *126*, 91−95.
(67) Breyer, E. D.; Strasters, J. K.; Khaledi, M. G. Quantitative Retention-Biological Activity Relationship Study by Micellar Liquid Chromatography. *Anal. Chem.* **1991**, *63* (8), 828−833.
(68) Le Paih, J.; Dérien, S.; Demerseman, B.; Bruneau, C.; Dixneuf, P. H.; Toupet, L.; Dazinger, G.; Kirchner, K. Ruthenium-Catalyzed Synthesis of Alkylidenecyclobutenes via Head-to-Head Dimerization of Propargylic Alcohols and Cyclobutadiene−Ruthenium Intermediates. *Chem.—Eur. J.* **2005**, *11* (4), 1312−1324.
(69) Migchels, P.; Zeegers-Huyskens, T. Infrared Study of the Proton Acceptor Ability of Metyrapone. *J. Phys. Org. Chem.* **1995**, *8* (2), 77−83.
(70) Sigala, P. A.; Kraut, D. A.; Caaveiro, J. M. M.; Pybus, B.; Ruben, E. A.; Ringe, D.; Petsko, G. A.; Herschlag, D. Testing Geometrical Discrimination within an Enzyme Active Site: Constrained Hydrogen Bonding in the Ketosteroid Isomerase Oxyanion Hole. *J. Am. Chem. Soc.* **2008**, *130* (41), 13696−13708.
(71) Yang, M.; Zhang, X. Comparative Developmental Toxicity of New Aromatic Halogenated DBPs in a Chlorinated Saline Sewage Effluent to the Marine Polychaete *Platynereis dumerilii*. *Environ. Sci. Technol.* **2013**, *47* (19), 10868−10876.
(72) McWhirter, C.; Lund, E. A.; Tanifum, E. A.; Feng, G.; Sheikh, Q. I.; Hengge, A. C.; Williams, N. H. Mechanistic Study of Protein Phosphatase-1 (PP1), a Catalytically Promiscuous Enzyme. *J. Am. Chem. Soc.* **2008**, *130* (41), 13673−13682.
(73) Chrystiuk, E.; Jusoh, A.; Santafianos, D.; Williams, A. Rate and Equilibrium Studies of the Reaction of Oxyanions with 2-Phenyloxazol-5(4*H*)-one. *J. Chem. Soc., Perkin Trans. 2* **1986**, No. 1, 163−168.
(74) Ragnar, M.; Lindgren, C. T.; Nilvebrant, N. O. pK(a)-Values of Guaiacyl and Syringyl Phenols Related to Lignin. *J. Wood Chem. Technol.* **2000**, *20* (3), 277−305.
(75) Fazary, A. E.; Ju, Y. H. Nonaqueous Solution Studies on the Protonation Equilibria of Some Phenolic Acids. *J. Solution Chem.* **2008**, *37* (9), 1305−1319.
(76) Nara, S. J.; Valgimigli, L.; Pedulli, G. F.; Pratt, D. A. Tyrosine Analogues for Probing Proton-Coupled Electron Transfer Processes in Peptides and Proteins. *J. Am. Chem. Soc.* **2009**, *132* (2), 863−872.

DOI: 10.1021/jp512996v
J. Phys. Chem. B XXXX, XXX, XXX−XXX